International Journal of Bio-Science and Bio-Technology
Vol.7, No.5 (2015), pp.65-84
http://dx.doi.org/10.14257/ijbsbt.2015.7.5.07

Effect of Couple Stress Fluid Flow on Magnetohydrodynamic Peristaltic Blood Flow with Porous Medium through Inclined Channel in the Presence of Slip Effect - Blood Flow Model

S. Ravi Kumar

Assistant Professor, Department of Mathematics
NBKR Institute of Science and technology, Vidyanagar, SPSR Nellore, Andhra Pradesh, India
drsravikumar1979@gmail.com / drsravikumar1979@nbkrist.org

Abstract

Effect of couple stress fluid flow on magnetohydrodynamic peristaltic blood flow with porous medium trough inclined channel in the presence of slip effect-Blood flow study have been studied under the assumption of long wavelength approximations. The expressions of the axial velocity, transverse velocity, pressure gradient, volume flow rate, average volume flow rate, pressure rise and shear stress are obtained and discussed through graphs. It is noted that the axial velocity increases with increase in M, S and α and deceases with increase in D and β and the transverse velocity increases with increase in D and S and decreases with increase in M, β and α in the entire flow field. We notice the pressure gradient is maximum at x = 0.5.

Keywords: *Couple stress fluid flow, peristaltic fluid flow, porous medium, magnetic field, slip condition and inclined channel*

1. Introduction

The word peristalsis stems from the Greek word Peristaltikos, which means clasping and compressing. Peristaltic pumping is a form of fluid transport generated in the fluid contained in a distensible tube when a progressive wave travels along the wall of the tube. It is an inherent property of many syncytial smooth muscle tubes, stimulation at any point can cause a contractile ring to appear in the circular muscle of the gut, and this ring then spreads along the tube. In addition, peristaltic pumping occurs in many practical applications involving biomechanical systems. This mechanism also finds many applications in roller and finger pumps, some bio-mechanical instruments, e.g. heart-lung machine, blood pump machine and dialysis machine. Thus, peristaltic transport has been the recent studies of many researchers/scientists owing to the above mentioned applications in bio-mechanical engineering and bio-medical technology. From the fluid mechanical point of view, peristaltic motion is characterized by the dynamic interaction of flexible boundary with the fluid. It was probably Latham [1] who first studied the mechanism of the peristalsis in relation to mechanical pumping. A number of analytical studies of peristaltic transport obtained by a train of periodic sinusoidal waves in an infinitely long two-dimensional symmetric channel or ax-symmetric tubes containing a Newtonian or non-Newtonian fluid with no-slip wall condition have been investigated in refs. [2-17]. It is now a well-accepted fact that the peristaltic flows of magnetohydrodynamic (MHD) fluids are important in medical sciences and bioengineering. The MHD characteristics are useful in the development of magnetic devices, cancer tumor treatment, and hyperthermia and blood reduction during surgeries. Hence several scientists having in mind such importance extensively discussed the peristalsis with magnetic field effects (Agarwal and Anwaruddin [18], Hayat and Ali [19], Mekheimer [20], Subba Reddy *et al.*, [21]).Since then, this work on magneto

ISSN: 2233-7849 IJBSBT

hydrodynamic (MHD) flow has received much attention. This is due to the fact that such studies are useful particularly for getting a proper understanding of the functioning of different machines used by clinicians for pumping blood (Misra *et al.*, [22]). Misra *et al.*, [23] pointed out that theoretical researches with an aim to explore the effect of a magnetic field on the flow of blood in atherosclerotic vessels also find application in a blood pump used by cardiac surgeons during the surgical procedure.

Couple stress fluids consist of rigid, randomly oriented particles suspended in a viscous medium. The couple stress fluid is a special case of the non-Newtonian fluids where these fluids are consisting of rigid randomly oriented particles suspended in a viscous medium and their sizes are taken into account. This model can be used to describe human and animal blood, infected urine from a diseased kidney and liquid crystals. From the recent attempts dealing with the couple stress model, we refer to Mekheimer [24], as he has investigated the problem of the peristaltic transport of a couple stress fluids in a uniform and non-uniform channel. Also Nadeem and Akram [25] have investigated the peristaltic flow of a couple stress fluids under the effect of induced magnetic field in an asymmetric channel, and Sobh [26] has studied the effect of slip velocity on peristaltic flow of a couple stress fluids in uniform and non-uniform channels. The peristaltic fluid flow through channels with flexible walls has been studied by Ravi Kumar *et al.*, [27-35]. Effects of induced magnetic field and slip condition on peristaltic transport with heat and mass transfer in a non-uniform channel has been studied by Najma Saleem *et al.*, [36].Couple stress fluid is known to be a better model for bio-fluids, such as blood, lubricants containing small amount of high polymer additive, electro-rheological fluids and synthetic fluids (Valanis and Sun [37]). The main feature of couple stress fluids is that the stress tensor is anti-symmetric and their accurate flow behavior cannot be predicted by the classical Newtonian theory. Stokes [38] generalized the classical model to include the effects of the presence of the couple stresses. Sankad and Radhakrishnamacharya [39], Srinivasacharya and Srikanth [40] and Mekheimer and Shehawey [41] studied the flow of couple stress fluid under different conditions.

2. Mathematical Formulation and Solution

We consider the peristaltic flow of a viscous incompressible Newtonian fluid with couple –stress through a porous a medium in magnetic field through a two-dimensional channel of non- uniform thickness with a sinusoidal wave travelling down its wall. A uniform magnetic field B_0 is applied in the transverse direction to the flow. The electrical conductivity of the fluid is assumed to be small so that the magnetic Reynolds number is small and the induced magnetic field is neglected in comparison with the applied magnetic field.

The geometry of the wall surface is defined as

$$h\ (x,t) = a(x) + b \sin\ \frac{2\pi}{\lambda}(x - ct) \qquad (1)$$

With $a(x) = a_0+kx$

where a(x) is the half-width of the channel at any axial distance x from inlet, a_0 is the half-width at inlet, k(<<1) is a constant whose magnitude depends on the length of the channel and exit and inlet dimensions, b is the wave amplitude,λ is the wave length, c is the propagation velocity and t is the time.

We introduce a wave frame of reference (*x*, *y*) moving with velocity *c* in which the motion becomes independent of time when the channel length is an integral multiple of the wave length and the pressure difference at the ends of the channel is a constant (Shapiro *et al.*, (1969)). The transformation from the fixed frame of reference (*X,Y)* to the wave frame of reference (*x*, *y*)is given by

x =X-ct, y = Y, u = U-c, v =V and p(x) = P(X, t),

where (u, v) and (U, V) are the velocity components, *p* and *P* are pressures in the wave and fixed frames of reference, respectively.

The equations governing the flow in wave frame of reference are given by

$$\frac{\partial u}{\partial x} + \frac{\partial v}{\partial y} = 0 \qquad (2)$$

$$\rho\left[\frac{\partial u}{\partial t} + u\frac{\partial u}{\partial x} + v\frac{\partial u}{\partial y}\right] = -\frac{\partial p}{\partial x} + \mu\left[\frac{\partial^2 u}{\partial x^2} + \frac{\partial^2 u}{\partial y^2}\right] - \left[\sigma B_0^{\,2}\right]u - \left[\frac{\mu}{k_1}\right]u + g\sin\alpha - \eta\nabla^4 u \qquad (3)$$

$$\rho\left[\frac{\partial v}{\partial t} + u\frac{\partial v}{\partial x} + v\frac{\partial v}{\partial y}\right] = -\frac{\partial p}{\partial y} + \mu\left[\frac{\partial^2 v}{\partial x^2} + \frac{\partial^2 v}{\partial y^2}\right] - \left[\sigma B_0^{\,2}\right]v - \left[\frac{\mu}{k_1}\right]v - g\cos\alpha \qquad (4)$$

u and v are the velocity components in the corresponding coordinates p is the fluid pressure, ρ is the density of the fluid, μ is the coefficient of the viscosity, η is the coefficient of couple stress, k_1 is the permeability of the porous medium, g is the acceleration due to gravity, inclination angle α and *k* is the thermal conductivity. Since it is presumed that the couple stress is caused by the presence of the suspending particles, obviously the clear fluid cannot support couple stress at the boundary, hence we have tactically assumed that, the components of the couple stress tensor at the wall vanish.

Using the following the non-dimensional variables

$$x^* = \frac{x}{\lambda},\quad y^* = \frac{y}{a_0}, u^* = \frac{u}{c}, v^* = \frac{\lambda v}{a_0 c}, p^* = \frac{a_0^{\,2} p}{\lambda\mu c}, t^* = \frac{c t}{\lambda}, \mathrm{Re} = \frac{\rho c a_0}{\mu}\quad M = \sqrt{\frac{\sigma}{\mu}}B_0 a_0$$

$$\delta = \frac{a_0}{\lambda}, \eta = \frac{a_0^{\,2} g}{\mu c},\quad \eta_1 = \frac{a_0^{\,3} g}{\lambda\mu c} \text{ and } h = 1 + \frac{\lambda k x}{a_0} + \phi\sin\{2\pi(x - t)\}$$

here ϕ (amplitude ratio) = $\frac{b}{a_0} < 1$

The equations governing the flow in wave frame of reference are given by

$$\frac{\partial u}{\partial x} + \frac{\partial v}{\partial y} = 0 \qquad (5)$$

$$\mathrm{Re}\,\delta\left[\frac{\partial u}{\partial t} + u\frac{\partial u}{\partial x} + v\frac{\partial u}{\partial y}\right] = -\frac{\partial p}{\partial x} + \delta^2\frac{\partial^2 u}{\partial x^2} + \frac{\partial^2 u}{\partial y^2} - s\delta^4\frac{\partial^4 u}{\partial x^4} - s\frac{\partial^4 u}{\partial y^4} - 2s\delta^2\frac{\partial^4 u}{\partial x^2\partial y^2}$$

$$-\frac{1}{D}u - M^2 u + \eta\sin\alpha \qquad (6)$$

$$\mathrm{Re}\,\delta\left[\frac{\partial v}{\partial t} + u\frac{\partial v}{\partial x} + v\frac{\partial v}{\partial y}\right] = -\frac{\partial p}{\partial y} + \delta^4\frac{\partial^2 v}{\partial y^2} + \delta^4\frac{\partial^2 v}{\partial y^2} + \delta^2\frac{\partial^2 v}{\partial y^2} - \delta^2\frac{1}{D}v - \delta^2 M^2 v - \eta_1\cos\alpha \qquad (7)$$

Using long wavelength (*i.e.*, $\delta << 1$) and negligible inertia (*i.e.*, $\mathrm{Re} \to 0$) approximations, we have

$$S\frac{\partial^4 u}{\partial y^4} - \frac{\partial^2 u}{\partial y^2} + \left[M^2 + \frac{1}{D}\right]u = -\left[\frac{\partial p}{\partial x} - \eta\sin\alpha\right] \qquad (8)$$

$$\frac{\partial p}{\partial y} = 0 \qquad (9)$$

With dimensionless boundary conditions

$$u = -\beta\frac{\partial u}{\partial y}, \frac{\partial^2 u}{\partial y^2} = 0 \quad \text{at} \quad y = h \quad (10)$$

$$\frac{\partial u}{\partial y} = 0 \, , \frac{\partial^3 u}{\partial y^3} = 0 \text{ at } \quad y = 0 \qquad (11)$$

Where β is the slip parameter

Solving equation (8) using the boundary conditions (10 and 11), we get

$$u = N_1 Cosh \ [\alpha_1 y] + N_2 Cosh \ [\alpha_2 y] - A \qquad (12)$$

Where $\alpha_1 = \sqrt{\frac{1 + \sqrt{1 - 4S(M^2 + \frac{1}{D})}}{2S}}$ $\alpha_2 = \sqrt{\frac{1 - \sqrt{1 - 4S(M^2 + \frac{1}{D})}}{2S}}$ $A = \left(\frac{\left(\frac{\partial p}{\partial x} - \eta \sin \alpha \right)}{\left(M^2 + \frac{1}{D} \right)} \right)$

$$N_1 = \left[\frac{-A \alpha_2^2 Cosh \ [\alpha_2 h]}{\alpha_1^2 Cosh \ [\alpha_1 h][Cosh \ [\alpha_2 h] + \beta \alpha_2 Sin \ h[\alpha_2 h]] - \alpha_2^2 Cosh \ [\alpha_2 h][Cosh \ [\alpha_1 h] + \beta \alpha_1 Sin \ h[\alpha_1 h]]} \right]$$

$$N_2 = \left[\frac{A \alpha_1^2 Cosh \ [\alpha_1 h]}{\alpha_1^2 Cosh \ [\alpha_1 h][Cosh \ [\alpha_2 h] + \beta \alpha_2 Sin \ h[\alpha_2 h]] - \alpha_2^2 Cosh \ [\alpha_2 h][Cosh \ [\alpha_1 h] + \beta \alpha_1 Sin \ h[\alpha_1 h]]} \right]$$

From equation (5)

$$v = B \ Sin \ h[\alpha_1 y] - C \ Sin \ h[\alpha_2 y] \qquad (13)$$

Where $B = \frac{A N_3}{\alpha_1}$ $C = \frac{A N_4}{\alpha_2}$ $N_3 = \frac{a\left[\alpha_2^3 Sinh \ [\alpha_2 h]\right] - \left[\alpha_2^2 Cosh \ [\alpha_2 h]\right]\left[\frac{\partial a}{\partial x}\right]}{a^2}$

$$N_4 = \frac{a\left[\alpha_1^3 Sinh \ [\alpha_1 h]\right] - \left[\alpha_1^2 Cosh \ [\alpha_1 h]\right]\left[\frac{\partial a}{\partial x}\right]}{a^2}$$

$$a = \alpha_1^2 Cosh \ [\alpha_1 h][Cosh \ [\alpha_2 h] + \beta \alpha_2 Sin \ h[\alpha_2 h]] - \alpha_2^2 Cosh \ [\alpha_2 h][Cosh \ [\alpha_1 h] + \beta \alpha_1 Sin \ h[\alpha_1 h]]$$

$$\frac{\partial a}{\partial x} =$$

$$\left(\alpha_1^2 Cosh \ [\alpha_1 h]\left(\alpha_2 Sinh \ [\alpha_2 h] + \beta \alpha_2^2 Cosh \ [\alpha_2 h]\right) + (Cosh \ [\alpha_2 h] + \beta \alpha_2 Sinh \ [\alpha_2 h])\alpha_1^3 Sinh \ [\alpha_1 h]\right) -$$

$$\left(\alpha_2^2 Cosh \ [\alpha_2 h]\left(\alpha_1 Sinh \ [\alpha_1 h] + \beta \alpha_1^2 Cosh \ [\alpha_1 h]\right) + (Cosh \ [\alpha_1 h] + \beta \alpha_1 Sinh \ [\alpha_1 h])\alpha_2^3 Sinh \ [\alpha_2 h]\right)$$

3. Shear Stress, Pressure Gradient and Pressure Rise

The shear stress at the upper wall y = h (x), in the dimensional form is given by

$$T = \frac{\frac{1}{2}\left[\frac{\partial u}{\partial y} + \frac{\partial v}{\partial x}\right]\left[1 - \left(\frac{dh}{dx}\right)^2\right] + \left[\frac{\partial v}{\partial y} - \frac{\partial u}{\partial x}\right]\left(\frac{dh}{dx}\right)}{\left[1 + \left(\frac{dh}{dx}\right)^2\right]}$$

and it's solution is given by

$$\tau = \left[\frac{\frac{1}{2}\left[[N_1 \alpha_1 \sinh[\ \alpha_1 y] + N_2 \alpha_2 \sinh[\ \alpha_2 y]] + \left[\left(\frac{\partial B}{\partial x}\right) \sinh[\ \alpha_1 y - \left(\frac{\partial C}{\partial x}\right) \sinh[\ \alpha_2 y \right] \right] \left[1 - h'^2\right]}{\left[1 + h'^2\right]} \right] +$$

$$\left[\frac{\left[\left[B\alpha_1 \cosh\left[\alpha_1 y\right] - C\alpha_2 \cosh\left[\alpha_2 y\right]\right] - \left[\left(\frac{\partial N_1}{\partial x}\right)\cosh\left[\alpha_1 y + \left(\frac{\partial N_2}{\partial x}\right)\cosh\left[\alpha_2 y\right]\right]\right]\left[h'\right]}{\left[1 + h'^2\right]}\right]$$

The rate of volume flow 'q' through each section is a constant (independent of both x and t).It is given by

$$q = \int_0^h u\, dy = \int_0^h \left(N_1 Cosh\left[\alpha_1 y\right] + N_2 Cosh\left[\alpha_2 y\right] - A\right) dy$$

$$= \frac{N_1}{\alpha_1} Sinh\left[\alpha_1 h\right] + \frac{N_2}{\alpha_2} Sinh\left[\alpha_2 h\right] - Ah \qquad (15)$$

Hence the flux at any axial station in the fixed frame is found to be given by

$$Q(x, t) = \int_0^h (u + 1) dy = q + h \qquad (16)$$

while the expression for the time-averaged volumetric flow rate over one period $T\left(=\frac{\lambda}{c}\right)$ of the peristaltic wave is obtained as

$$\overline{Q} = \frac{1}{T}\int_0^T Q dt = q + 1 \quad (17)$$

The pressure gradient obtained from equation (17) can be expressed as

$$\frac{dp}{dx} = \left(\frac{\left(M^2 + \frac{1}{D}\right)(\overline{Q} - 1)}{(-a_1 Sinh\left[\alpha_1 h\right] + a_2 Sinh\left[\alpha_2 h\right] - h)}\right) + \eta \sin\alpha \quad (18)$$

Where

$$a_1 = \left[\frac{\alpha_2^2 Cosh\left[\alpha_2 h\right]}{\alpha_1\left(\alpha_1^2 Cosh\left[\alpha_1 h\right]\left[Cosh\left[\alpha_2 h\right] + \beta\alpha_2 Sin\, h\left[\alpha_2 h\right]\right] - \alpha_2^2 Cosh\left[\alpha_2 h\right]\left[Cosh\left[\alpha_1 h\right] + \beta\alpha_1 Sin\, h\left[\alpha_1 h\right]\right]\right)}\right]$$

$$a_2 = \left[\frac{\alpha_1^2 Cosh\left[\alpha_1 h\right]}{\alpha_2\left(\alpha_1^2 Cosh\left[\alpha_1 h\right]\left[Cosh\left[\alpha_2 h\right] + \beta\alpha_2 Sin\, h\left[\alpha_2 h\right]\right] - \alpha_2^2 Cosh\left[\alpha_2 h\right]\left[Cosh\left[\alpha_1 h\right] + \beta\alpha_1 Sin\, h\left[\alpha_1 h\right]\right]\right)}\right]$$

The pressure rise Δ_{P_L} (at the wall) in the channel of length L, non-dimensional form is given by

$$\Delta_p = \int_0^1 \frac{dp}{dx} dx$$

$$\Delta_p = \int_0^1 \left[\left(\frac{\left(M^2 + \frac{1}{D}\right)(\overline{Q} - 1)}{(-a_1 Sinh\left[\alpha_1 h\right] + a_2 Sinh\left[\alpha_2 h\right] - h)}\right) + \eta \sin\alpha\right] dx$$

4. Numerical Results and Discussion

The analytical expressions for the axial velocity, transverse velocity, shear stress, pressure gradient and pressure rise have been derived in the last section. The numerical and computational results are discussed through the graphical illustration. **Mathematica** software is used to find out numerical results. The axial and transverse velocities are

presented in the figures (1) to (20) for various in the governing parameters like couple stress parameter (S), porous parameter (D),magnetic field (M) and slip parameter (β) and inclined angle (α).The effects of *D*on axial velocity are shown in Figures 1 and 2. From these figures, it can be seen that the axial velocity (u) decreases with increasing the Porous parameter (D) with M ≥ 0.1 for fixed S = 0.1, β = 0.2, η = 0.5, $\alpha = \frac{\pi}{6}$, $\frac{dp}{dx}$ = 0.5, ϕ = 0.7, x = t= $\frac{\pi}{4}$, λ = 10, k = 0.0005, a_0= 0.01. Figures 3 and 4 illustrate the effects of magnetic field on axial velocity (u).It is interested to note that the axial velocity rapidly increases with increase in magnetic field (M) with D ≥1for fixed S = 0.1, β = 0.2, η = 0.5, $\alpha = \frac{\pi}{6}$, $\frac{dp}{dx}$ = 0.5, ϕ = 0.7, x = t= $\frac{\pi}{4}$, λ = 10, k = 0.0005, a_0= 0.01.The axial velocity distribution (u) with Couple stress parameter (S) as depicted in Figures (5) to (6) with M ≥ 0.1for being fixed other parameters. We observe that the axial velocity increases with increase in Magnetic field (M). Figures 7 and 8 are plotted to study the effect of β on the velocity. We observed that the velocity gradually decreases with increase in β with M ≥ 0.1 for fixed S = 0.1, β = 0.2, η = 0.5, $\alpha = \frac{\pi}{6}$, $\frac{dp}{dx}$ = 0.5, ϕ = 0.7, x = t= $\frac{\pi}{4}$, λ = 10, k = 0.0005, a_0= 0.01. The effects of α on axial velocity are depicted in Figures 9 and 10. We observe that that the axial velocity enhances with enhance in inclined angle α with D ≥1 for fixed M = 0.5, S = 0.1, η = 0.5, $\frac{dp}{dx}$ = 0.5, ϕ = 0.7, x = t = $\frac{\pi}{4}$, λ = 10, k = 0.0005, a_0= 0.01. Hence we conclude that the axial velocity increases with increase in M, S and α and deceases with increase in D and β throughout the flow field.

The transverse velocity distribution (v) with porous parameter (D) as depicted in Figures (11) to (12) with M ≥ 0.1. We notice that the transverse velocity enhances with increase in porous parameter (D) for fixed S = 0.1, β = 0.2, η = 0.5, $\alpha = \frac{\pi}{6}$, $\frac{dp}{dx}$ = 0.5, ϕ = 0.7, x = t= $\frac{\pi}{4}$, λ = 10, k = 0.0005, a_0= 0.01. From Figures 13 and 14, We notice that the transverse velocity (v) decreases with increase in Magnetic field (M) with D ≥1for fixed S = 0.1, β = 0.2, η = 0.5, $\alpha = \frac{\pi}{6}$, $\frac{dp}{dx}$ = 0.5, ϕ = 0.7, x = t= $\frac{\pi}{4}$, λ = 10, k = 0.0005, a_0= 0.01. Figures 15 and 16 reveal the transverse velocity (v) with Couple stress parameter (S). We observe that the transverse velocity (v) enhances with increase in S with M ≥ 01for fixed other parameters. The effects of β on transverse axial velocity are depicted in Figures 17 and 18. We observe that the transverse velocity (v) decreases with increase in slip parameter (β) with M ≥ 0.1 for fixed S = 0.1, β = 0.2, η = 0.5, $\alpha = \frac{\pi}{6}$, $\frac{dp}{dx}$ = 0.5, ϕ = 0.7, x = t= $\frac{\pi}{4}$, λ = 10, k = 0.0005, a_0= 0.01. Figures 19 and 20 illustrate the effect of α on transverse axial velocity (v).We notice that the transverse velocity decreases with increase in α. Hence we conclude that the transverse velocity increases with increase in D and S and decreases with increase in M, β and α. Figures 21 to 28 reveals the axial pressure gradient for different value of S, M, D, α and β. Figures 20 and 21 illustrate the influence of $\overline{Q}$ on pressure gradient dp/dx. The figures show that the wider part of the channel $x \varepsilon [0,0.3]$ and $x \varepsilon [0.7,1]$, the pressure gradient is relatively small. Hence, the flow can easily pass without imposing large pressure gradient. However, in the narrow part of channel $x \in$ [0.3, 0.7], larger pressure gradient is needed to maintain the same flux to pass through it and we notice that the pressure gradient is increases with increase in $\overline{Q}$. The

effects of Mon pressure gradient dp/dx are shown in Figures 23 and 24. We notice that the magnitude of dp/dx is inversely proportional to M and notice that pressure gradient is maximum at x = 0.5. Figures 25-26 illustrate the variations of $\frac{dp}{dx}$ with S. From these figures, it can be seen that the axial pressure gradient is decreases with increase in S. From the figures, we observed that through the region $x\varepsilon[0.2,0.8]$ *i.e.*, narrowing part of the channel, the flow cannot pass easily. Therefore, it required large pressure gradient to maintain the same flux to pass it in the narrow part of the channel. The effects of D on axial pressure gradient are depicted in figures 27 and 28.It is interested to note that the pressure gradient is increases with increase in D and notice that pressure gradient is maximum at x = 0.5. Figure 29 to 30 reveals the behavior of the shear stress in a cycle of oscillations at different points of wave length for various in governing parameters S, D, M, α and β. We notice that no separation occurs in flow field.

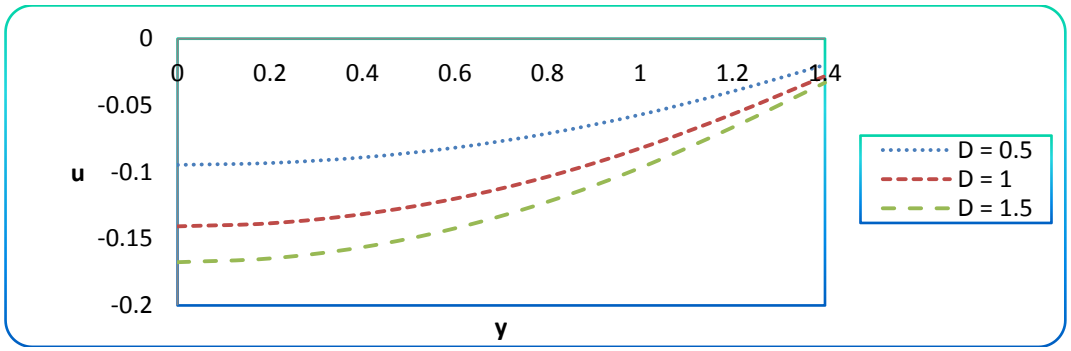

Figure 1. Distribution of Axial Velocity for Different Values of D with fixed M = 0.1, S = 0.1, β = 0.2, η = 0.5, $\alpha = \frac{\pi}{6}$, $\frac{dp}{dx}$ **= 0.5,** ϕ **= 0.7, x = t =** $\frac{\pi}{4}$, λ **= 10, k = 0.0005, a_0= 0.01**

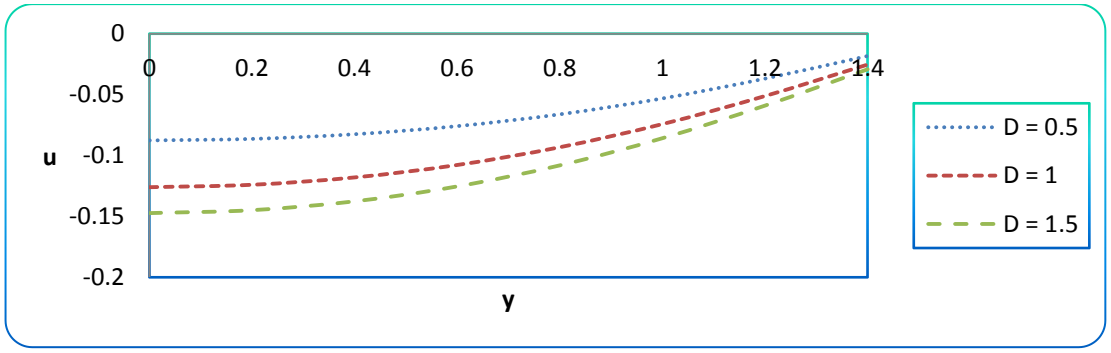

Figure 2. Distribution of Axial Velocity for Different Values of D with Fixed M = 0.5,S = 0.1, β = 0.2, η = 0.5, $\alpha = \frac{\pi}{6}$, $\frac{dp}{dx}$ **= 0.5,** ϕ **= 0.7, x = t =** $\frac{\pi}{4}$, λ **= 10, k = 0.0005, a_0= 0.01**

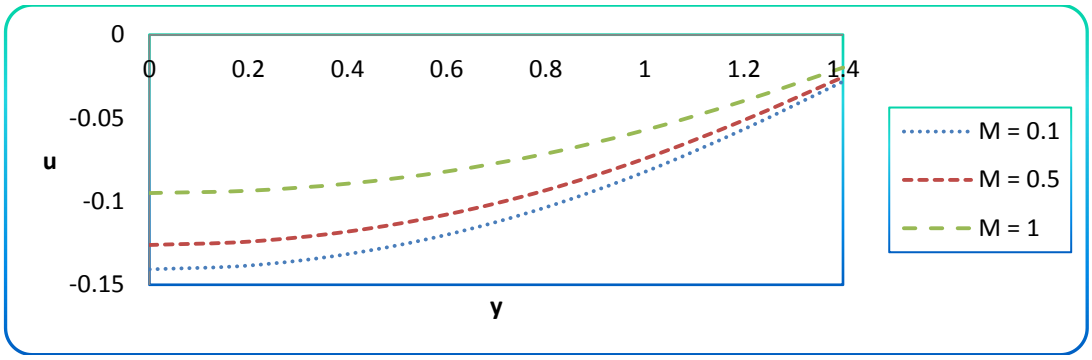

Figure 3. Distribution of Axial Velocity for Different Values of M with Fixed D = 1,S = 0.1, β = 0.2, η = 0.5, $\alpha = \frac{\pi}{6}$, $\frac{dp}{dx}$ = 0.5, ϕ = 0.7, x = t = $\frac{\pi}{4}$, λ = 10, k = 0.0005, a_0= 0.01

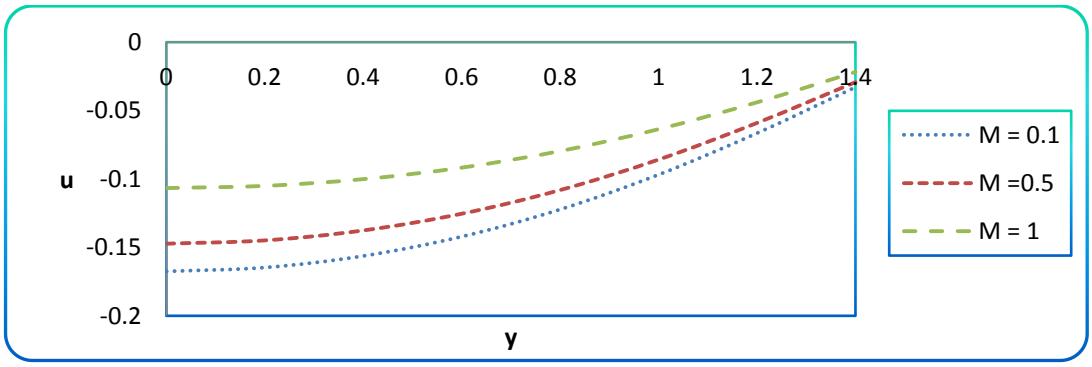

Figure 4. Distribution of Axial Velocity for Different Values of M with Fixed D = 1.5, S = 0.1, β = 0.2, η = 0.5, $\alpha = \frac{\pi}{6}$, $\frac{dp}{dx}$ = 0.5, ϕ = 0.7, x = t = $\frac{\pi}{4}$, λ = 10, k = 0.0005, a_0= 0.01

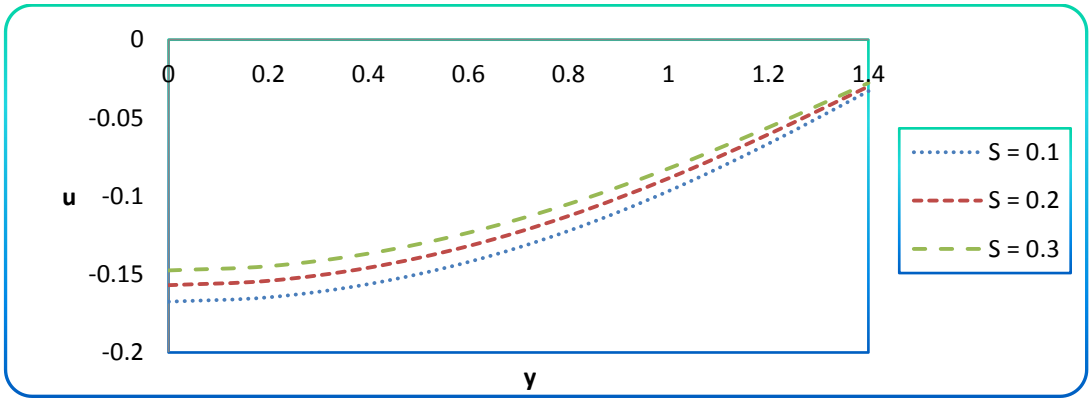

Figure 5. Distribution of Axial Velocity for Different Values of S with Fixed D = 1.5, M = 0.1, β = 0.2, η = 0.5, $\alpha = \frac{\pi}{6}$, $\frac{dp}{dx}$ = 0.5, ϕ = 0.7, x = t = $\frac{\pi}{4}$, λ = 10, k = 0.0005, a_0= 0.01

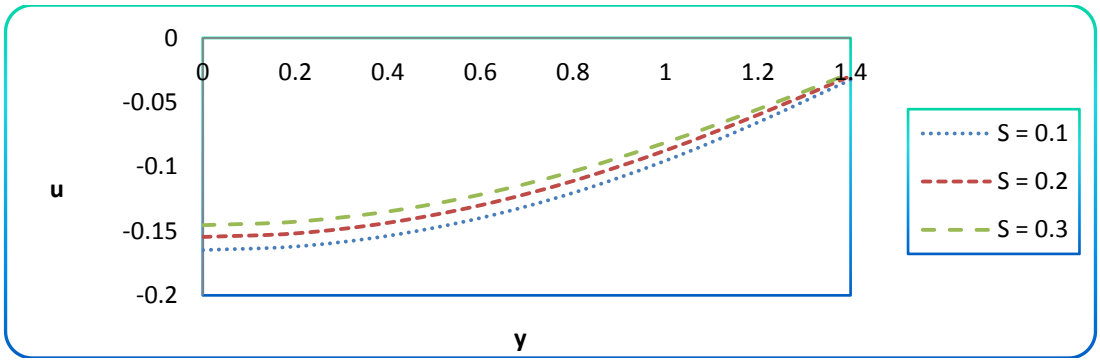

Figure 6. Distribution of Axial Velocity for Different values of S with Fixed D = 1.5, M = 0.5, β = 0.2, = η 0.5, $\alpha = \frac{\pi}{6}$, $\frac{dp}{dx}$ = 0.5, ϕ = 0.7, x = t = $\frac{\pi}{4}$, λ = 10, k = 0.0005, a_0= 0.01

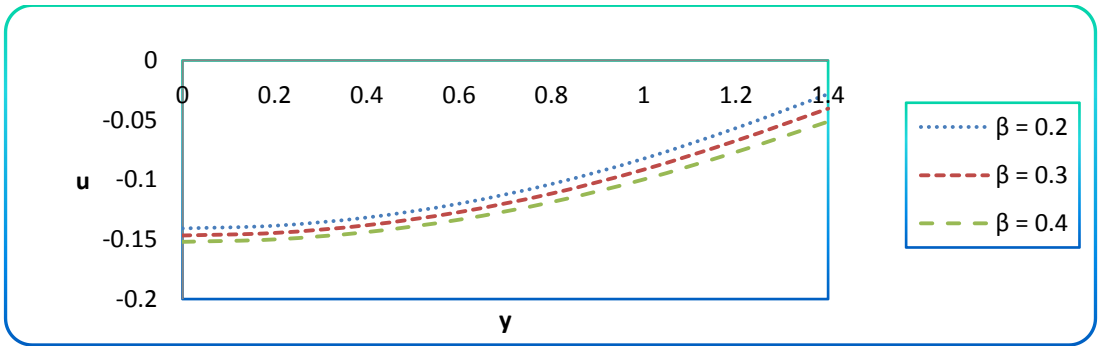

Figure 7. Distribution of Axial Velocity for Different Values of β with Fixed D = 1, M = 0.1, S = 0.1, η = 0.5, $\alpha = \frac{\pi}{6}$, $\frac{dp}{dx}$ = 0.5, ϕ = 0.7, x = t = $\frac{\pi}{4}$, λ = 10, k = 0.0005, a_0= 0.01

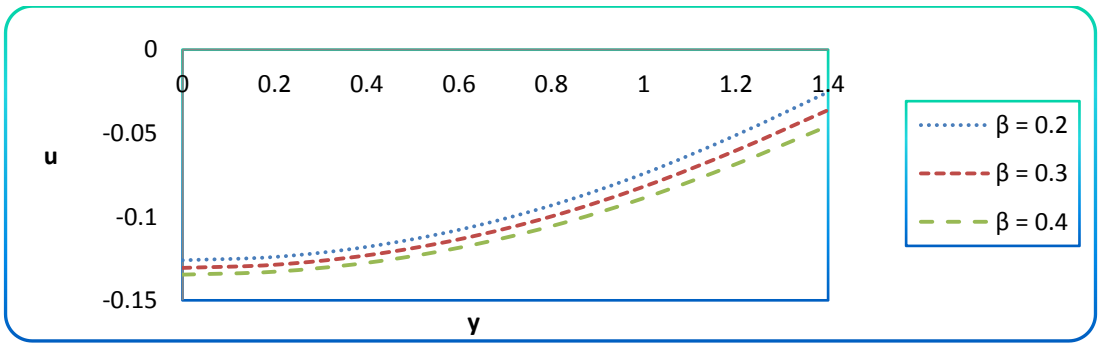

Figure 8. Distribution of Axial Velocity for Different Values of β with Fixed D = 1, M = 0.5, S = 0.1, η = 0.5, $\alpha = \frac{\pi}{6}$, $\frac{dp}{dx}$ = 0.5, ϕ = 0.7, x = t = $\frac{\pi}{4}$, λ = 10, k = 0.0005, a_0= 0.01

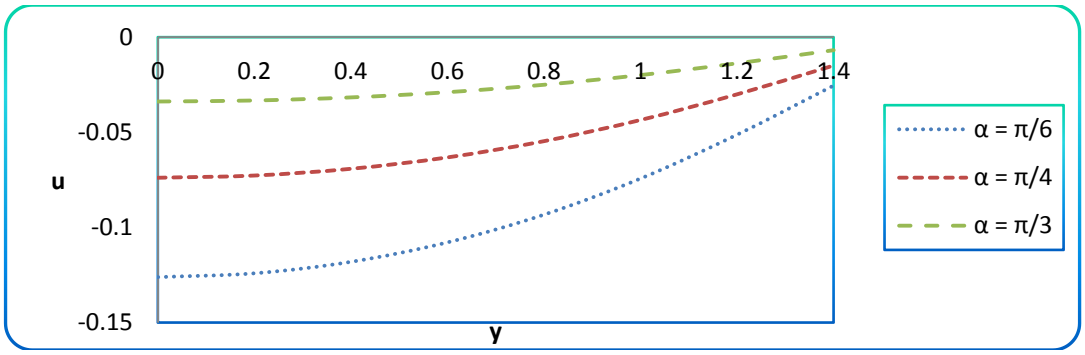

Figure 9. Distribution of Axial Velocity for Different Values of α with Fixed D = 1, M = 0.5, S = 0.1, η = 0.5, $\frac{dp}{dx}$ = 0.5, ϕ = 0.7, x = t = $\frac{\pi}{4}$, λ = 10, k = 0.0005, a_0= 0.01

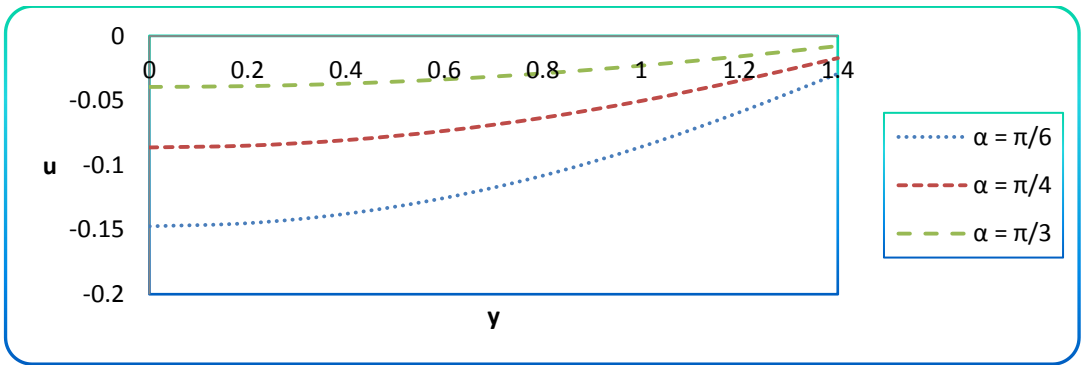

Figure 10. Distribution of Axial Velocity for Different Values of α with Fixed D = 1.5, M = 0.5, S = 0.1, η = 0.5, $\frac{dp}{dx}$ = 0.5, ϕ = 0.7, x = t = $\frac{\pi}{4}$, λ = 10, k = 0.0005, a_0= 0.01

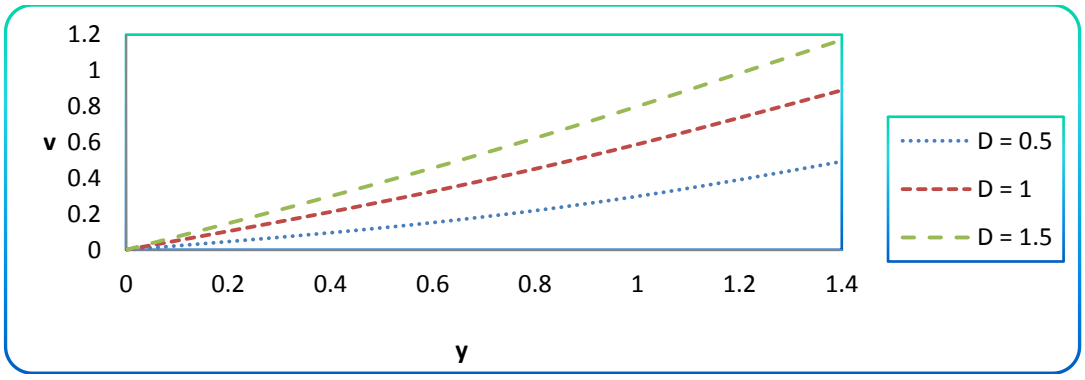

Figure 11. Distribution of Transverse Velocity for Different Values of D with Fixed M = 0.1, S = 0.1, β = 0.2, η = 0.5, $\alpha = \frac{\pi}{6}$, $\frac{dp}{dx}$ = 0.5, ϕ = 0.7, x = t = $\frac{\pi}{4}$, λ = 10, k = 0.0005, a_0= 0.01

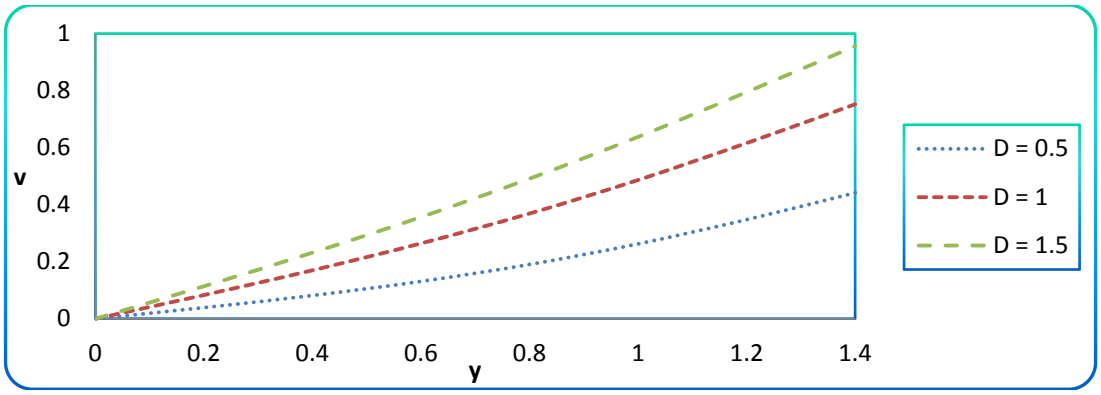

Figure 12. Distribution of Transverse Velocity for Different Values of D with Fixed M = 0.5, S = 0.1, β = 0.2, η = 0.5, $\alpha = \frac{\pi}{6}$, $\frac{dp}{dx}$ = 0.5, ϕ = 0.7, x = t = $\frac{\pi}{4}$, λ = 10, k = 0.0005, a_0= 0.01

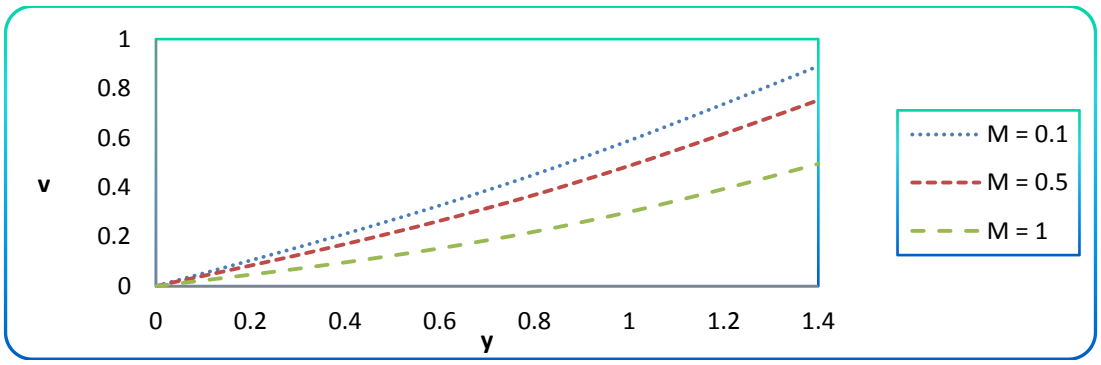

Figure 13. Distribution of Transverse Velocity for Different Values of M with Fixed D = 1, S = 0.1, β = 0.2, η = 0.5, $\alpha = \frac{\pi}{6}$, $\frac{dp}{dx}$ = 0.5, ϕ = 0.7, x = t = $\frac{\pi}{4}$, λ = 10, k = 0.0005, a_0= 0.01

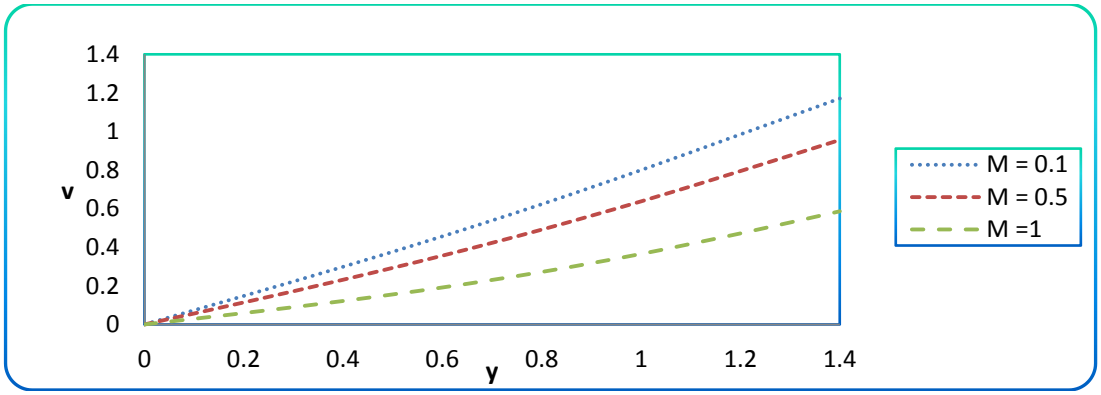

Figure 14. Distribution of Transverse Velocity for Different Values of M with Fixed D = 1.5, S = 0.1, β = 0.2, η = 0.5, $\alpha = \frac{\pi}{6}$, $\frac{dp}{dx}$ = 0.5, ϕ = 0.7, x = t = $\frac{\pi}{4}$, λ = 10, k = 0.0005, a_0= 0.01

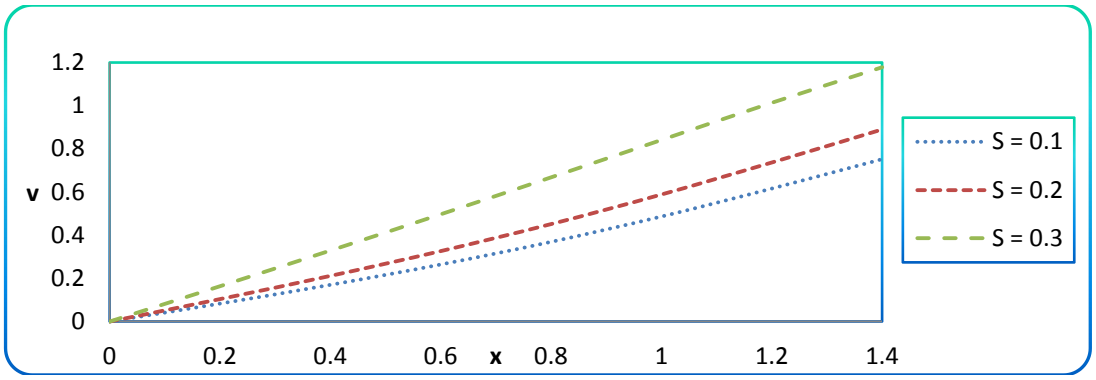

Figure 15. Distribution of Transverse Velocity for Different Values of S with Fixed D = 1.5, M = 0.1, β = 0.2, η = 0.5, $\alpha = \frac{\pi}{6}$, $\frac{dp}{dx}$ = 0.5, ϕ = 0.7, x = t = $\frac{\pi}{4}$, λ = 10, k = 0.0005, a_0= 0.01

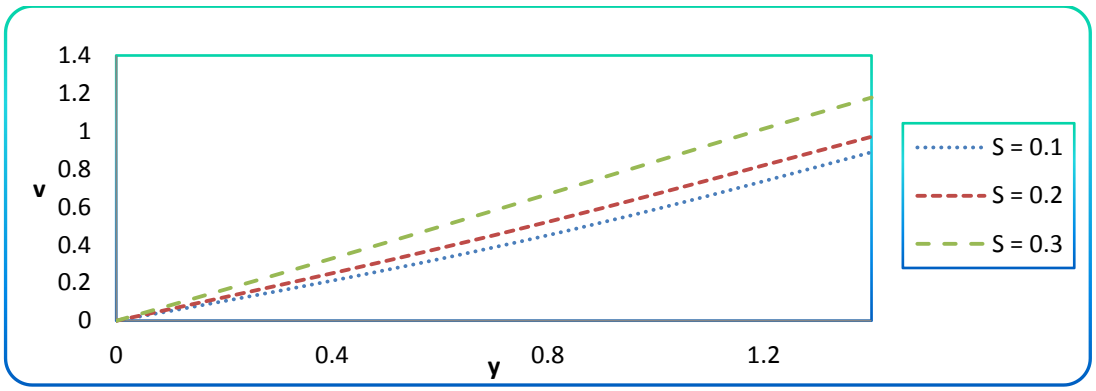

Figure 16. Distribution of Transverse Velocity for Different Values of S with Fixed D = 1.5, M = 0.5, β = 0.2, η = 0.5, $\alpha = \frac{\pi}{6}$, $\frac{dp}{dx}$ = 0.5, ϕ = 0.7, x = t = $\frac{\pi}{4}$, λ = 10, k = 0.0005, a_0= 0.01

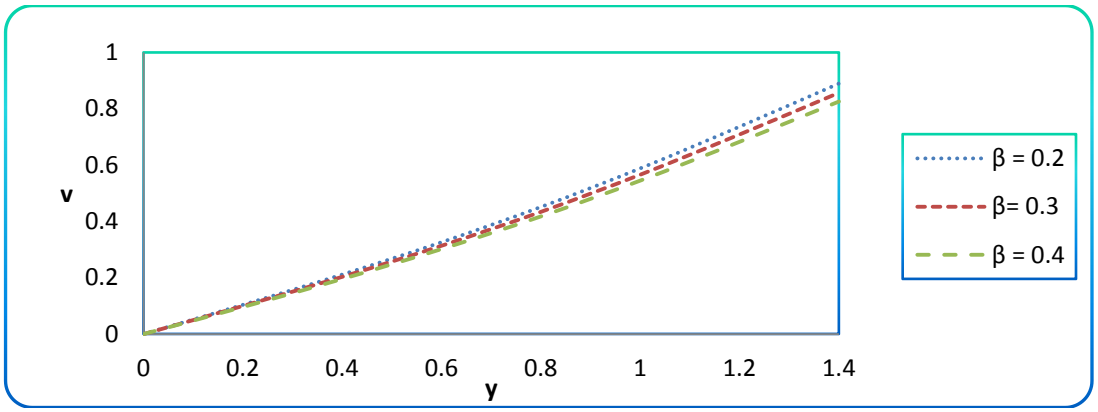

Figure 17. Distribution of Transverse Velocity for Different Values of β with fixed D = 1, M = 0.1, S 0.1, η = 0.5, $\alpha = \frac{\pi}{6}$, $\frac{dp}{dx}$ = 0.5, ϕ = 0.7, x = t = $\frac{\pi}{4}$, λ = 10, k = 0.0005, a_0= 0.01

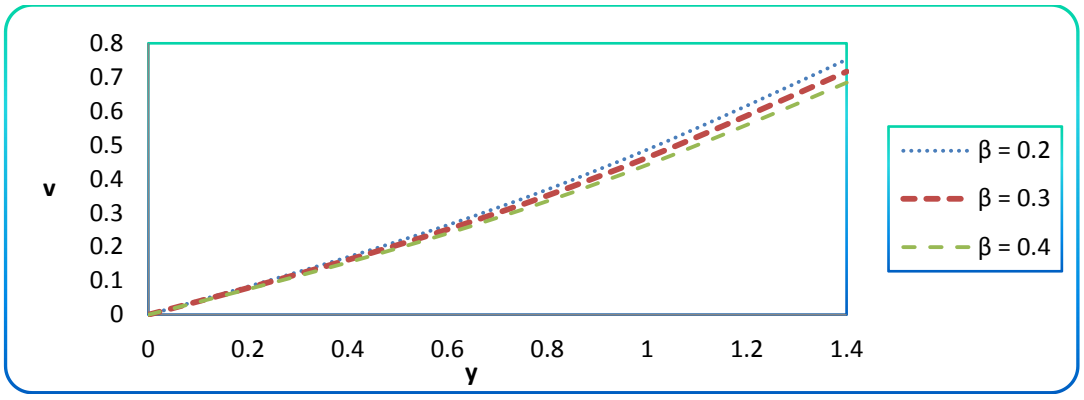

Figure 18. Distribution of Transverse Velocity for Different Values of β with Fixed D = 1, M = 0.5, S = 0.1, η = 0.5, $\alpha = \frac{\pi}{6}$, $\frac{dp}{dx}$ = 0.5, ϕ = 0.7, x = t = $\frac{\pi}{4}$, λ = 10, k = 0.0005, a_0= 0.01

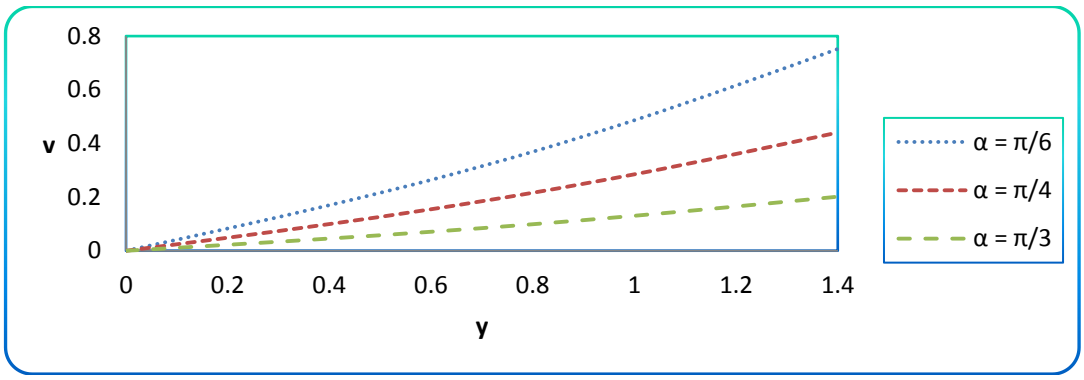

Figure 19. Distribution of Transverse Velocity for Different Values of α with Fixed D = 1, M = 0.5, S = 0.1, η = 0.5, $\frac{dp}{dx}$ = 0.5, ϕ = 0.7, x = t = $\frac{\pi}{4}$, λ = 10, k = 0.0005, a_0= 0.01

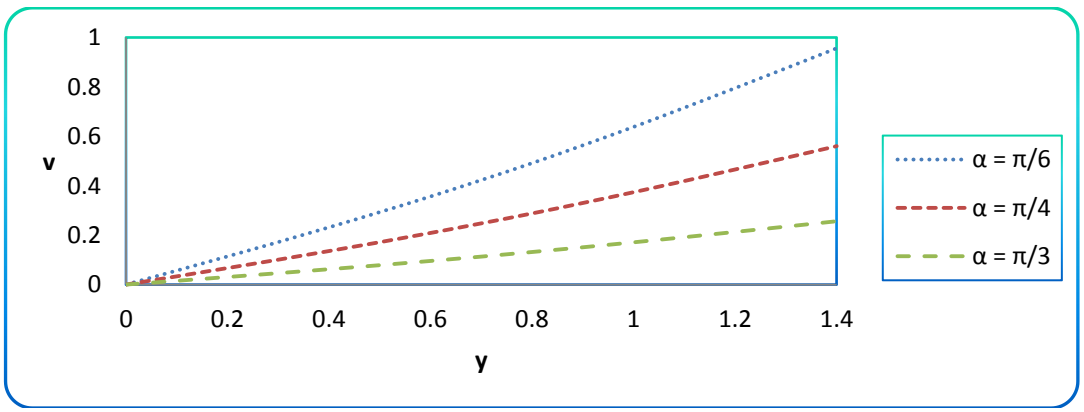

Figure 20. Distribution of Transverse Velocity for Different Values of α with Fixed D = 1.5, M = 0.5, S = 0.1, η = 0.5, $\frac{dp}{dx}$ = 0.5, ϕ = 0.7, x = t = $\frac{\pi}{4}$, λ = 10, k = 0.0005, a_0= 0.01

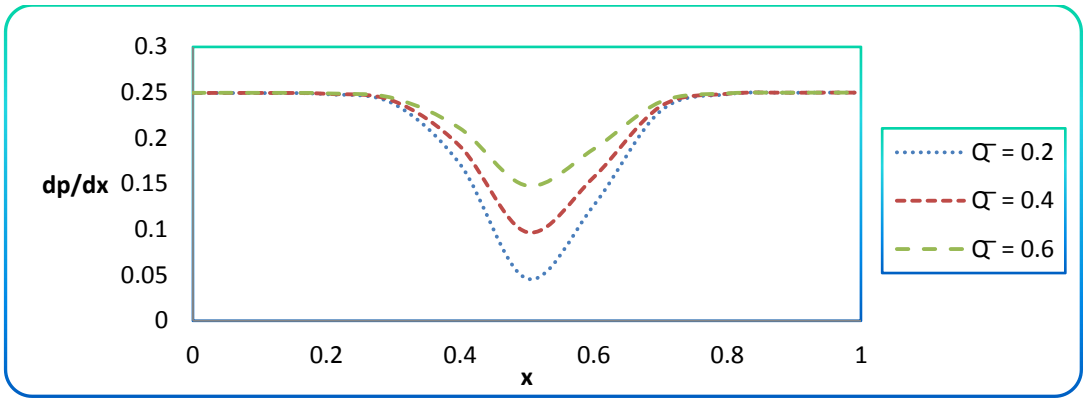

Figure 21. Distribution of Pressure Gradient Versus x with $\bar{Q}$ for Fixed D = 1.5, M = 0.1, S = 0.3, β = 0.2, η = 0.5, $\alpha = \frac{\pi}{6}$, ϕ = 0.7, t = $\frac{\pi}{4}$, λ = 10, k = 0.0005, a_0= 0.01

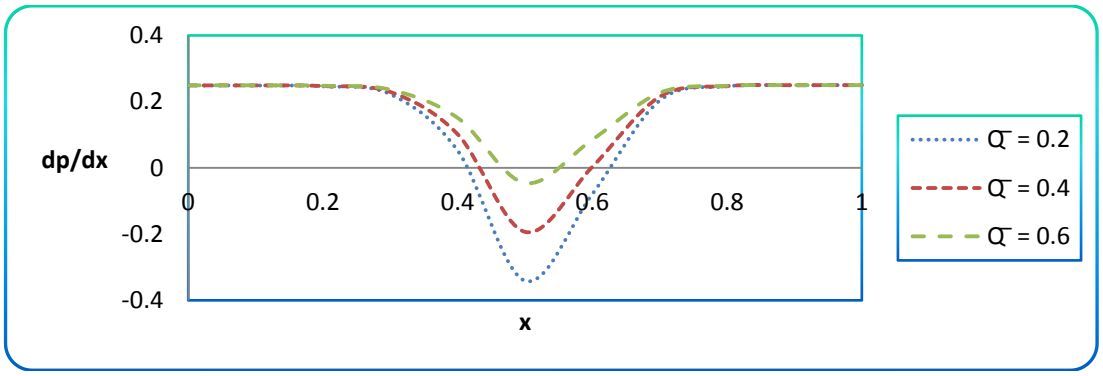

Figure 22. Distribution of Pressure Gradient Versus x with $\bar{Q}$ for Fixed D = 1.5, M = 0.3, S = 0.3, β = 0.2, η = 0.5, $\alpha = \frac{\pi}{6}$, ϕ = 0.7, t = $\frac{\pi}{4}$, λ = 10, k = 0.0005, a_0= 0.01

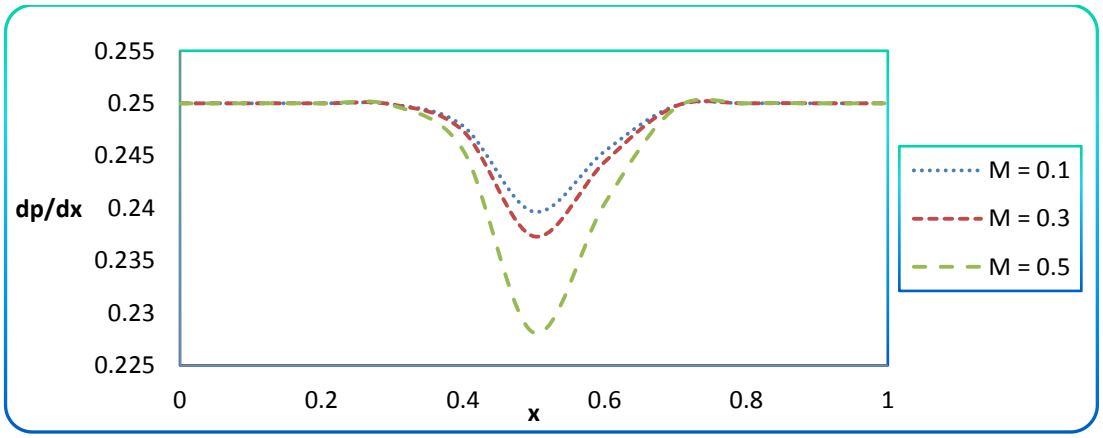

Figure 23. Distribution of Pressure Gradient Versus x with M for Fixed D = 0.5, S = 0.1,β = 0.2, $\bar{Q} = 0.2$, η = 0.5, $\alpha = \frac{\pi}{6}$, ϕ = 0.7, t = $\frac{\pi}{4}$, λ = 10, k = 0.0005, a_0= 0.01

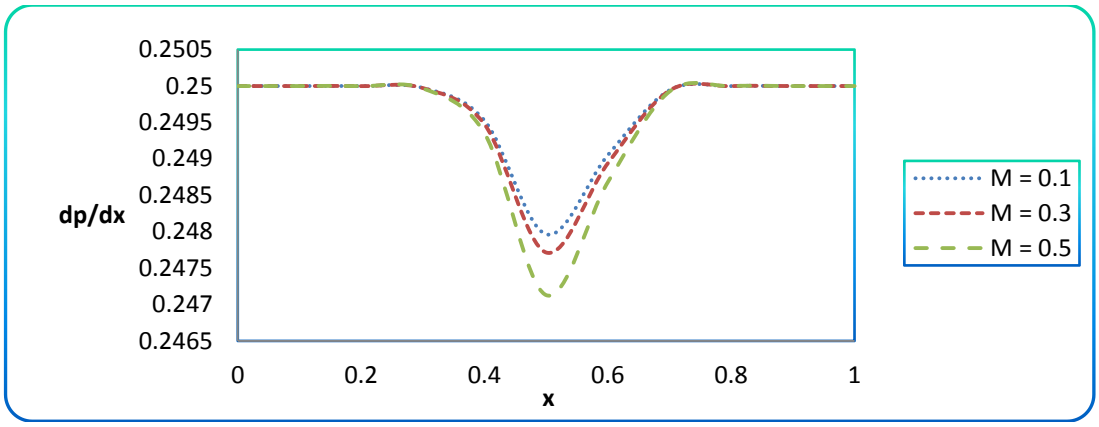

Figure 24. Distribution of Pressure Gradient Versus x with M for Fixed D = 1, S = 0.1,β = 0.2,$\bar{Q} = 0.2$, η = 0.5, $\alpha = \frac{\pi}{6}$, ϕ = 0.7, t =$\frac{\pi}{4}$, λ = 10, k = 0.0005, a_0= 0.01

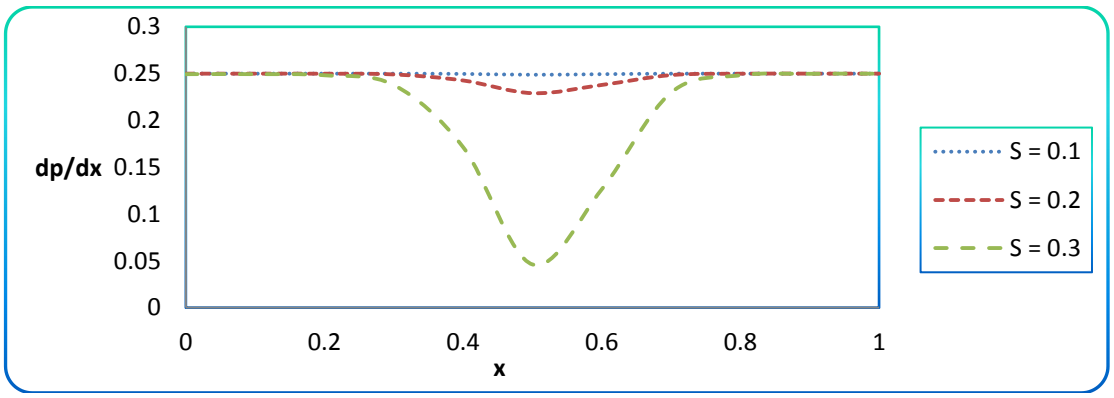

Figure 25. Distribution of Pressure Gradient Versus x with S for Fixed D = 1.5, M = 0.1, β = 0.2, $\bar{Q} = 0.2$, η = 0.5, $\alpha = \frac{\pi}{6}$, ϕ = 0.7, t =$\frac{\pi}{4}$, λ = 10, k = 0.0005, a_0= 0.01

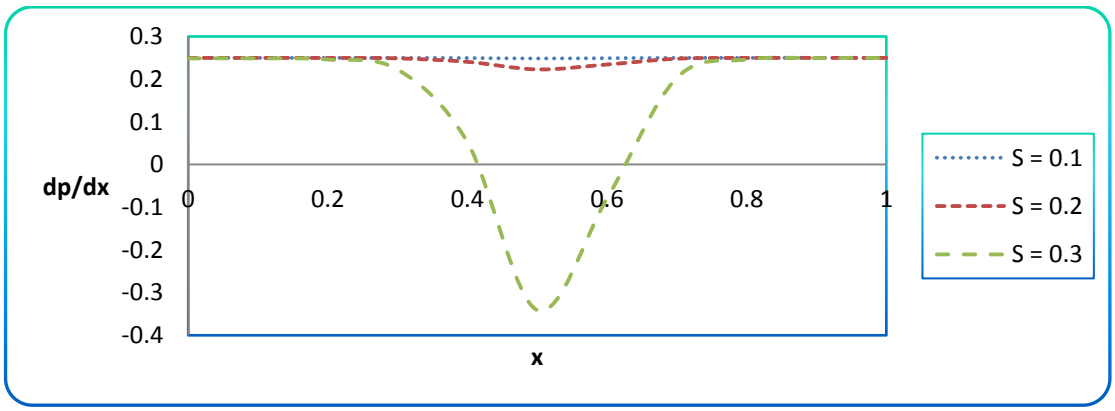

Figure 26. Distribution of Pressure Gradient Versus x with S for Fixed D = 1.5, M = 0.3, β = 0.2, $\bar{Q} = 0.2$, η = 0.5, $\alpha = \frac{\pi}{6}$, ϕ = 0.7, t =$\frac{\pi}{4}$, λ = 10, k = 0.0005, a_0= 0.01

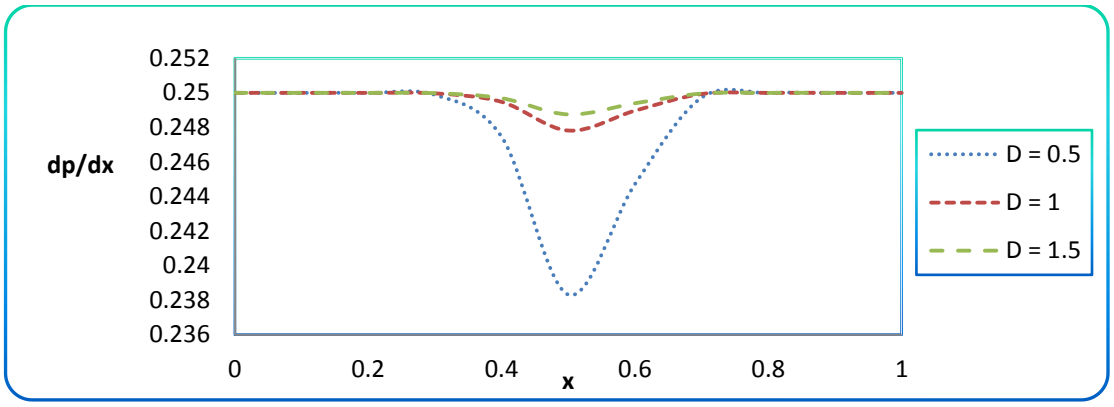

Figure 27. Distribution of Pressure Gradient Versus x with D for Fixed S = 0.1, M = 0.1, β = 0.2, $\bar{Q} = 0.2$, η = 0.5, $\alpha = \frac{\pi}{6}$, ϕ = 0.7, t = $\frac{\pi}{4}$, λ = 10, k = 0.0005, a_0= 0.01

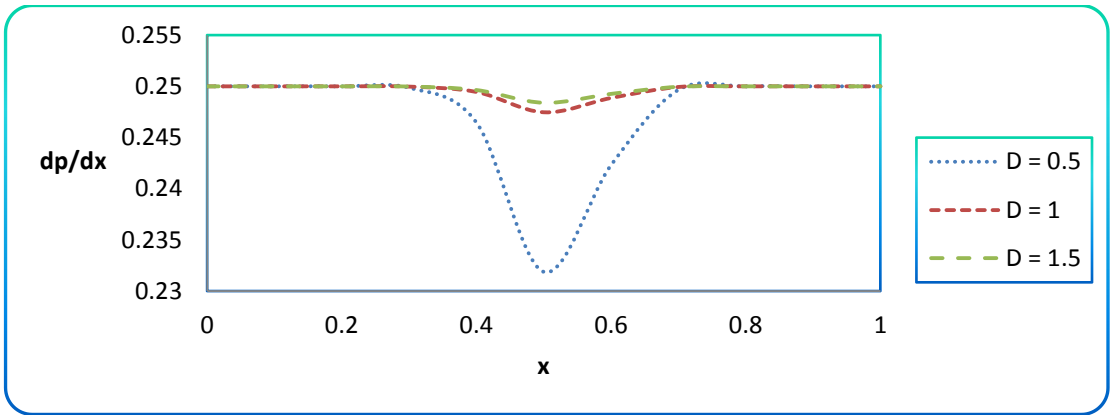

Figure 28. Distribution of Pressure Gradient versus x with D for Fixed S = 0.1, M = 0.5, β = 0.2, $\bar{Q} = 0.2$, η = 0.5, $\alpha = \frac{\pi}{6}$, ϕ = 0.7, t = $\frac{\pi}{4}$, λ = 10, k = 0.0005, a_0= 0.01

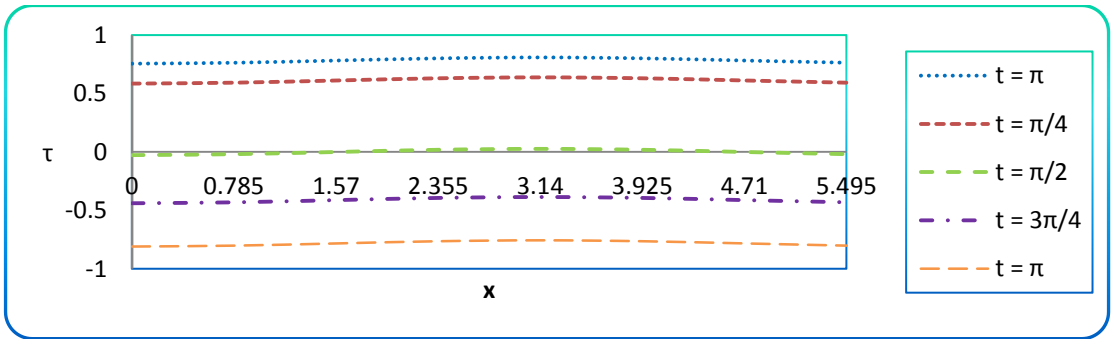

Figure 29. Distribution of Shear Stresses τ for S = 0.1, M = 0.1, D = 1, β = 0.2, $\bar{Q} = 0.2$, η = 0.5, $\alpha = \frac{\pi}{6}$, ϕ = 0.7, t = $\frac{\pi}{4}$, λ = 10, k = 0.0005, a_0= 0.01

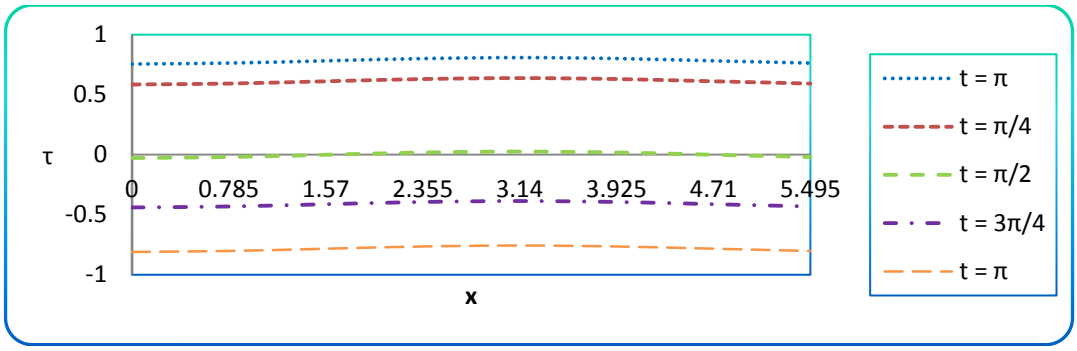

Figure 30. Distribution of Shear Stresses τ for S = 0.1, M = 0.1, D = 1.5, β = 0.2,$\bar{Q} = 0.2$, η = 0.5, $\alpha = \frac{\pi}{6}$, ϕ = 0.7, t = $\frac{\pi}{4}$, λ = 10, k = 0.0005, a_0= 0.01

5. Conclusions

Effect of couple stress fluid flow on magnetohydrodynamic peristaltic blood flow with porous medium trough inclined channel in the presence of slip effect-Blood flow study is investigated under the assumption of long wavelength approximation. Furthermore, the effect of various values of parameters on axial velocity, transverse velocity, pressure gradient and shear stress have been computed numerically and explained graphically. We conclude the following observations:

1. The axial velocity increases with increase in M, S and α and deceases with increase in D and β.
2. The transverse velocity increases with increase in D and S and decreases with increase in M, β and α in the entire flow field.
3. The pressure gradient is maximum at x = 0.5.
4. The pressure gradient is decreases with increase in S.
5. The pressure gradient is increases with increase in$\bar{Q}$.

Acknowledgements

We would like to thank to the reviewers and editors for their encouraging comments and constructive suggestions to improve the manuscript.

References

[1] T. W. Lathem, "Fluid motion in a peristaltic pump", Master's thesis, Massachusetts, MIT, Cambridge, **(1966)**.
[2] A. E. H. Abd El Naby and A. E. M. El Misiery, "Effects of an endoscope and generalized Newtonian fluid on peristaltic motion", J. Applied Mathematics and Computation, vol. 128, **(2002)**, pp. 19-35.
[3] G. B. Bohme and R. Friedrich, "Peristaltic flow of viscoelastic liquids", J.Fluid Mech, vol. 128**, (1983),** pp. 109-122.
[4] A. E. M. El Misery, A.E.H. Abd El Naby and El A.H. Nagar, "Effects of fluid with variable viscosity and an endoscope on peristaltic motion", Phys. Soc. Jpn, vol. 72, no. 1, **(2003)**, pp. 89-94.
[5] E. F. Elshehawey and K.S. Mekheimer, "Couple-Stresses in peristaltic transport of fluids", J. Phys. D: Appl. Phys, vol. 27, **(1994)**, pp. 1163-1170.
[6] A. M. Elshehawey, A. E. M. El Misery and A. A. Hakeem, "Peristaltic motion of generalized Newtonian fluid in a non-uniform channel", J. Phys. Soc. Jpn., vol. 67, **(1998)**, pp. 434-440.
[7] Y. C. Fung and C. S. Yih, "Peristaltic transport", J. Appl.Mech., vol. 35, **(1968)**, pp. 669-675.
[8] B. B. Gupta and V. Seshadri, "Peristaltic pumping in uniform tubes", Biomechanics**, (1976)**, pp. 105-109.
[9] H. S. Lew, Y. C. Fung, and C. B. Lowenstein, "Peristaltic carrying and mixing of chime", Biomech, vol. 4, **(1971)**, pp. 297-315.
[10] A. M. Provost and W. H. Schwarz, "A theoretical study of viscous effects in peristaltic pumping", Fluid Mech., vol. 279, **(1994)**, pp. 177-195.
[11] C. Pozrikidis, "A study of peristaltic flow", Fluid Mech., vol. 180, **(1987)**, pp. 515-527.

[12] A. H. Shapiro, M. Y. Jaffrin and S. L. Weinberg, "Peristaltic pumping with long wavelengths at low Reynolds number", Fluid Mech., vol. 37, **(1969)**, pp. 799-825.
[13] J. B. Shukla, R. S. Parihar, B. R. P. Rao and S. P. Gupta, "Effects of peripheral layer viscosity on peristaltic transport of a bio-fluid", Fluid Mech., vol. 37, **(1980)**, pp. 799-825.
[14] A. M. Siddiqui and W. H. Schwarz, "Peristaltic motion of a second-order fluid in tubes", Non-Newtonian Fluid Mech., vol. 53**, (1994)**, pp. 257-284.
[15] L. M. Srivastava and V. P. Srivastava, "Peristaltic transport of a blood: Casson model-II", Biomech., vol. 17, **(1984)**, pp. 821-829.
[16] L. M. Srivastava and V. P. Srivastava, "Peristaltic transport of a non- Newtonian fluid: Applications to the vas deferens and small intestine", Annals of Bio-Engng., vol. 13, **(1985)**, pp. 137-153.
[17] L. M. Srivastava and V. P. Srivastava, "Peristaltic transport of a powerlaw fluid: Applications to the ducts efferents of the reproductive tract", Rheological Acta, vol. 275, **(1988)**. pp. 428-433.
[18] H. L. Agarwal and B. Anwaruddin, "Peristaltic flow of blood in a branch", Ranchi University Math., vol. 15, **(1984)**, pp. 111.
[19] T. Hayatand N. Ali, "Peristaltically induced motion of a MHD third grade fluid in a deformable tube", Physica A: Statistical Mechanics and its applications, vol. 370, **(2006)**, pp. 225-239.
[20] Kh. S. Mekheimer, "Peristaltic flow of blood under effect of a magnetic field in a non-uniform channel", Appl. Math. Comput, vol. 153, **(2004)**, pp. 763-777.
[21] M. V. Subba Reddy, B. Jaya Rami Reddy, M. Sudhakar Reddy and N. Nagendra, "Long wavelength approximation to MHD peristaltic flow of a Bingham fluid through a porous medium in an inclined channel", International Journal of Dynamics of Fluids, vol. 7, no. 2, **(2011)**, pp. 157-170.
[22] J. C. Misra and S. Chakravarty, "Flow in arteries in the presence of stenosis", Journal of Biomech., vol. 19, **(1986)**, pp. 907-918.
[23] J. C. Misra, S. Maiti and G. C. Shit, "Peristaltic Transport of a Physiological Fluid in an Asymmetric Porous Channel in the Presence of an External Magnetic Field", Journal of Mechanics in Medicine and Biology, vol. 8, **(2008)**, pp. 507-525.
[24] Kh. S. Mekheimer, "Peristaltic transport of a couple stress fluid in a uniform and non-uniform channels", Biorehology, vol. 39, **(2002)**, pp. 755-765.
[25] S. Nadeem and S. Akram, "Peristaltic flow of a couple stress fluid under the effect of induced magnetic field in an asymmetric channel", Arch. Appl. Mech., vol. 81, **(2011)**, pp. 97-109.
[26] A. M. Sobh, "Interaction of couple stresses and slip flow on peristaltic transport in uniform and non-uniform channels", Turkish J. Eng. Env. Sci., vol. 32, **(2008)**, pp. 117-123.
[27] S. Ravikumar, G. Prabhakara Rao and R. Siva Prasad, "Peristaltic flow of a couple stress fluid flows in a flexible channel under an oscillatory flux", Int. J. of Appl. Math and Mech., vol. 6, no. 13, **(2010)**, pp. 58-71.
[28] S. Ravikumar and R. Siva Prasad, "Interaction of pulsatile flow on the peristaltic motion of couple stress fluid through porous medium in a flexible channel", Eur. J. Pure Appl. Math, vol. 3, **(2010)**, pp. 213-226.
[29] S. Ravikumar, "Peristaltic Fluid Flow Through Magnetic Field At Low Reynolds Number In A Flexible Channel Under An Oscilatory Flux", International journal of Mathematical Archive, vol. 4, no. 1, **(2013)**, pp. 36-52.
[30] S. Ravikumar, G. Prabhakara Rao and R. Siva Prasad, "Peristaltic flow of a second order fluid in a flexible channel', Int. J. of Appl. Math and Mech., vol. 6, no. 18, **(2010)**, pp. 13-32.
[31] S. Ravikumar, "Peristaltic transportation with effect of magnetic field in a flexible channel under an oscillatory flux", Journal of Global Research in Mathematical Archives, vol. 1, no. 5, **(2013)**, pp. 53-62.
[32] S. Ravikumar, "Hydromagnetic Peristaltic Flow of Blood with Effect of Porous Medium through coaxial vertical Channel: A Theoretical Study", International Journal of Engineering Sciences & ResearchTechnology, vol. 2, no. 10, **(2013)**, pp. 2863-2871.
[33] S. Ravikumar, G. Prabhakara Rao and R. Siva Prasad, "Hydromagnetic two-phase viscous ideal fluid flow in a parallel plate channel under a Pulsatile pressure gradient", International Journal of Fluid mechanics Research, vol. 39, no. 4, **(2012)**,pp. 291-300.
[34] S. Ravikumar and A. Ahmed, "Magnetohydrodynamic couple Stress Peristaltic flow of blood Through Porous medium in a Flexible Channel at low Reynolds number", Online International Interdisciplinary Research Journal, vol. III, no. VI, **(2013)**, pp. 157-166.
[35] S. Ravikumar, "Peristaltic flow of blood through coaxial vertical channel with effect of magnetic field: Blood flow study", International Journal of Recent advances in Mechanical Engineering (IJMECH), vol. 3, no. 4, **(2014)**, pp. 85-96.
[36] N. Saleem, T. Hayat and A. Alsaedi, "Effects of induced magnetic field and slip condition on peristaltic transport with heat and mass transfer in a non-uniform channel", International Journal of the Physical Sciences, vol. 7, no. 2, pp. 191-204, **(2012)** January 9.
[37] K. C. Valanis and C. T. Sun, "Poiseuille flow of a fluid with couple stress with applications to blood flow", Biorheology, vol. 6, **(1969)**, pp. 85-97.
[38] V. K. Stokes, "Couple Stresses in Fluids", Phys. Fluids, vol. 9, **(1966)**, pp. 1709-1715.
[39] G. C. Sankad and G. Radhakrishnamacharya, "Effect of Magnetic field on the peristaltic transport of couple stress fluid in a channel with wall properties", Int. J. Biomath., vol. 4, **(2011)**, pp. 365-378.

[40] D. Srinivasacharya and D. Srikanth, "Effect of couple stresses on the pulsatile flow through a constricted annulus", Comptus Rendus Mecanique, vol. 336, **(2008)**, pp. 820-827.
[41] Kh. S. Mekheimer and E. F. El. Shehawey, "Couple stresses in peristaltic transport of fluids", Phys. D: Appl. Phys., vol. 27, **(1994)**, pp. 1163-1170.

Author

Dr. S. Ravi Kumar, has done B.Sc. (Mathematics) from Sri Krishna Devaraya University, Anantapur, India in 1999, M.Sc (Mathematics) from Sri Venkateswara University, Tirupati, India in 2002, M.Phil (Fluid Mechanics) from Sri Krishna Devaraya University, Anantapur, India in 2006 and Ph.D (Fluid Mechanics) from Sri Krishna Devaraya University, Anantapur, India in 2009. He has published more than 20 papers in International / National Journals. His research areas of interest are Peristaltic fluid flows, Couple stress fluid flows, Heat and Mass Transfer, MHD fluid flows and Fluid Dynamics.